Synthesis, Characterization and Antimicrobial Activity of Copper-Nickel Bimetallic Metal Organic Framework

*JAYASREE KOMARA [1], JAYA PRASANTHI KARUMURI [1, *], SUNIL KUMAR SWABHI [2]*

[1]Department of Chemistry, Andhra University, Visakhapatnam, Andhra Pradesh, 530003, India

[2]Department of Engineering Chemistry, Andhra University, Visakhapatnam, Andhra Pradesh, 530003, India

Abstract

Copper-Nickel bimetallic metal organic framework (Cu-Ni-EDTA) sample was synthesized using a solvothermal technique. The powder was dried and analysed using FTIR, XRD, FESEM-EDS, TGA, XPS and BET. Thermogravimetric Analysis (TGA) was used to determine the thermal stability of the product. On the other hand, this sample's morphology and surface area were determined using FESEM and BET analysis, respectively. The bioactivity of the sample was determined by measuring the inhibitory zone diameter surrounding the samples (mm). The characterization results showed that on the IR spectra, a series of absorption peaks at 481,678, 1396, 1459, 1605 and 1654 cm^{-1} was identified indicating the formation of Cu-Ni-EDTA bimetallic MOF (BMOF). X-ray patterns of the prepared sample exhibit sharp peaks at 16.3º, 32.4º and 39.8º that correspond to BMOF. The BMOF thermogram demonstrated three stages: moisture and ethanol evaporation, DMF solvent evaporation, and breakdown of the organic linker, resulting in CuO and NiO as end products. The sample's bioactivity was tested against three bacterial strains: Salmonella typhi (MTCC-8767), Escherichia coli (MTCC-443) and Staphylococcus aureus (MTCC-3160). The results demonstrated that BMOF is an excellent antibacterial agent against the three bacterial strains listed above.

Keywords: Copper-Nickel-Ethylenediaminetetraacetate (Cu-Ni-EDTA); Metal Organic Framework (MOF); Cu-Ni-EDTA Bimetallic MOF (BMOF); Escherichia coli (E.coli); Salmonella typhi (S.typhi); Staphylococcus aureus (S.aureus)

1. Introduction

The most difficult issue in human history has been antibacterial contamination. Because it helps us against antimicrobial infection and maintain our health, sanitation is vitally important. The necessity of proper hygiene and sanitation was demonstrated by the recent global Corona virus disease (Covid-19) pandemic [1]. Humans have created a number of techniques and protocols over the ages to combat different types of infections. More than half of the world's population, or 4.2 billion people, still lack access to proper sanitation in terms of both environmental and human health, although recent advancements [2]. The existence of pathogens that cause disease, such as bacteria, viruses, fungus, and other microorganisms, makes sanitation necessary. In order to safeguard people from illnesses spread by harmful microbes, all disinfection procedures must include the elimination of microorganisms [3]. Numerous techniques and substances have been created to enhance the effectiveness of eliminating these microbes. Chlorine, alcohol, heat treatment, monochloramine, and chlorine dioxide are the ingredients of standard disinfection techniques. Modern techniques, on the other hand, make use of photochemical disinfectants, hydrogen peroxide, ozone, UV light, and electrochemical therapy [4].

Tens of millions of cases and more than 100,000 deaths from typhoid fever, a human disease caused by Salmonella Typhi (S. Typhi), are reported to occur annually in low- and middle-income countries (LMICs). S. Typhi is rarely found in environments with extensive access to clean water, sanitation, and hygiene infrastructure. Instead, it is predominantly transferred by the faecal-oral pathway, which is

typically contaminated food and water. Typhoid fever is therefore most common in Africa and South and Southeast Asia. Typhoid fever episodes are clinically characterized by bacteraemia and a variety of symptoms that can make it challenging to differentiate the illness from other febrile illnesses. Severe instances may result in gastrointestinal perforation, sepsis, and even death [5]. Escherichia coli (E. coli) is the causative agent of numerous human diseases, such as septicaemia, extraintestinal illnesses, newborn meningitis, diarrhoea, and urinary tract infections [6]. Furthermore, Staphylococcus aureus (S. aureus) is the causative agent of a number of illnesses, including eye infections, pneumonia, infective endocarditis, septicaemia, and infections of the central nervous system [7]. Antimicrobial resistance impacts both animals and humans and is an international threat to health. This is due in part to the growing likelihood that the genes causing resistance will be transferred between different bacterial genera, which could lead to treatment failure, higher medical costs, animal deaths, and financial losses [8]. It has been reported that by 2050, antimicrobial-resistant bacteria could kill up to 10 million people [9].

Metal–organic frameworks (MOFs) are among the greatest materials to have evolved in the biomedical field. Because of their distinct form and particular chemical and physical characteristics, which can effectively kill bacteria through physical interaction and the gradual release of metal ions, they have the potential to be long-lasting antimicrobial and biocompatible [10]. As organic linkers between the metal nodes, bipedal or multimodal organic ligands give MOFs their porosity, low-density crystalline structure [11]. MOFs have been extensively studied and used in a variety of fields, including adsorption and separation, gas storage, organo-catalysis, sensing, photocatalysis, the field of electrochemistry and contaminant removal from water or gas. These fields have been attracted to MOFs due to their numerous high specific surface area, coordination-unsaturated metal sites, tuneable substitutable components and tuneable porous structure [12]. Their applications in biology and medicine have grown as a result of their excellent simplicity of functionalization, biodegradability and low toxicity [13]. Furthermore, MOF is a perfect material for a variety of antibacterial applications in the field of biomedicine due to its strong interaction with bacterial membranes, production of ROS under irradiation, controlled/stimulated decomposition, high loading amounts and controlled release of other antibacterial agents [10,13]. Furthermore, because MOFs have higher drug loadings than other materials, they can serve as effective carriers for the regulated delivery of active ingredients [14]. The release of bioactive metal ions or ligands into the media following the breakage of metal–ligand bonds is the general mechanism by which bioactive MOFs function [15]. It has been proposed that second metal ions be inserted into framework nodes to form bimetallic MOFs, which would boost the catalytic, electrical, luminous, etc. capabilities of MOFs. Due to the partial replacement of second metal ions in the secondary-building units (SBUs) or inorganic nodes of the framework, the bimetallic system exhibits synergistic effects. Bimetallic MOFs' physicochemical characteristics can be changed by adjusting or even controlling the metal ratios in the material [16]. Catalysis, gas adsorption, luminescence detection, energy conversion, and storage are only a few of the areas where bimetallic MOFs with adjustable compositions and structures perform better than their monometallic counterparts [17]. Numerous techniques, such as direct synthesis, one-pot synthesis, template synthesis, post-synthetic modification, post-synthetic exchange and seed-induced growth, can be used to create bimetallic MOFs. The primary components that have been found to have a substantial impact on MOFs' capacity to sterilize bacteria through inactivation are metal ions and ligands. The antibacterial mechanism of MOFs has also been hypothesized in recent years. Because of the superior physical-chemical properties of MOF materials, they are able to effectively combat antibiotic drug resistance [18] and exhibit strong antibacterial activity. The main mechanisms they rely on are hydrophobic and electrostatic interactions between MOFs and bacteria, as well as van der Waals forces [19]. MOFs can also be employed as a metal storage container for the gradual release of Co, Zn, Cu, Ag, and Ni ions in addition to having a persistent antibacterial activity [20]. Released metal ions have the ability to gradually pierce cell membranes and demolish cell components. The activation processes of various metal ions vary. Other metals that may have antibacterial qualities, like Cu and Ni, have been the subject of recent research [21].

Many Cu-Ni Bimetallic MOFs have been synthesized, including $Ni_x Cu_{(3-x)} (HITP)_2$ MOFs [22], Ni-Cu-BTC [23], Ni-Cu-BDC [24] and so on. EDTA served as the ligand in the production of the Ni-Cu bimetallic MOF. To the best of my knowledge, this is the first published literature on the Cu-Ni-EDTA

Bimetallic MOF (BMOF). The synthesized Ni-Cu bimetallic MOF is further characterized by Fourier Transform Infrared Spectroscopy (FT-IR), Powder X-ray Diffraction (PXRD), Field Emission Scanning Electron Microscopy-Energy Dispersive X-ray Spectroscopy (FESEM-EDS), Brunauer-Emmett-Teller (BET), X-ray Photoelectron Spectroscopy (XPS) and Thermogravimetric Analysis (TGA).

2. Experimental section

2.1. Materials

All of the chemicals were used without further purification; they were purchased from reputable companies like Coastal Chemicals and Sigma-Aldrich Chemicals. A.R. grade ethanol was employed to wash the Cu-Ni-EDTA Bimetallic MOF. The water used to make the solutions has undergone double distillation. Every piece of glassware was carefully washed and rinsed with double-distilled water to remove any chance of contamination. It was then dried in an oven before being used.

2.2. Synthesis of Cu-Ni-EDTA Bimetallic MOF (BMOF)

First, use a digital weighing balance to precisely weigh two milligrams of copper nitrate trihydrate, two milligrams of nickel chloride hexahydrate, and two milligrams of the disodium salt of ethylenediamine tetra acetic acid. Next, pour the ingredients that have been weighted into a 100ml reagent vial. Five millilitres of double-distilled water should be added to the reagent bottle to dissolve its contents. Dimethyl formamide (DMF), 35 millilitres, should now be added to the mixture. Measure and record the pH of the solution using a pH paper. The pH of the solution must be in the range of 6 to 8. If not, adjust the pH by adding 0.1N CH_3COOH or 0.1N NaOH. To create a transparent solution, mix the contents of the reagent bottle for 120 minutes using a hotplate and magnetic stirrer. Initially green, the fluid gradually turns blue. Once the reagent bottle is filled, put it in the hot air oven and heat it to 150°C for ten hours. After ten hours, the 100ml reagent bottle needs to be taken out of the hot air oven. After taking the 100 ml reagent vial out of the hot air oven, centrifuge the precipitate. Wash the residue four to five times with double-distilled water and then four to five times with ethanol to remove any pollutants that may have dissolved in water or an organic solvent. Pulverize the residue to a fine powder after allowing it to dry in a hot air oven at 70°C for the entire night.

2.3. Test microorganisms

To assess the antibacterial activity, overnight growth at 37°C was performed on bacterial cultures of Salmonella typhi (MTCC-8767), Escherichia coli (MTCC-443) and Staphylococcus aureus (MTCC-3160). These cultures were kept in recently made nutrient agar slants after being obtained from the Microbial Type Culture Collection (MTCC) and Gene Bank, Institute of Microbial Technology (IMTECH), Chandigarh, India. The organisms were kept for extended periods of time at -20ºC with 15% v/v glycerol.

2.4. Muller-Hinton agar medium(1L)

39 grams of the commercially available Nutrient Medium were dissolved in 1000 millilitres of distilled water to create the medium. The dissolved media was thoroughly mixed, autoclaved for 15 minutes at 121°C and 15 pounds of pressure, and then poured, still molten, onto 100 mm Petri plates (25–30 mL/plate).

2.5. Nutrient broth(1L)

Thirteen grams of commercially available Nutrient Agar Medium were dissolved in one litre of distilled water by boiling the medium to complete dissolution. After being dispensed as needed, the medium was autoclaved for 15 minutes at 15 pounds of pressure (121 degrees Celsius).

2.6. Characterizations

For the powder-XRD measurements, the Bruker D8 Advance X-Ray Diffractometer was used; for the FT-IR, the Bruker alfa-II; for the FESEM-EDS, the Quanta FEG 250; for the TGA, the Hitachi STA 7300 model; for the XPS, the AXIS SUPRA X-Ray Photoelectron Spectrometer and for the BET analysis using N_2 isotherms at 77 K, the Quantachrome NOVA touch 4 LX instrument was utilized.

3. Results and discussions

3.1. Fourier transform infrared spectroscopy (FT-IR)

As seen in Figure 1, the synthesized Cu-Ni-EDTA Bimetallic MOF's FT-IR spectra were obtained in the 4000-400 cm^{-1} range. The peak located at 481.9 cm^{-1} represents the stretching and bending modes of Cu-O. The asymmetric stretching vibrations of carboxylate are indicated by the peaks at 1605 and 1654 cm^{-1}, whereas the symmetric vibrations are indicated by the large absorption bands at 1396.9 and 1459.3 cm^{-1} [25]. One of the distinctive vibration peaks of Ni-O was the absorption peak, which was located at 678.68 cm^{-1}. The C-N bond has been identified as the absorption band in EDTA chelates, located between 1070 and 1100 cm^{-1} [26].

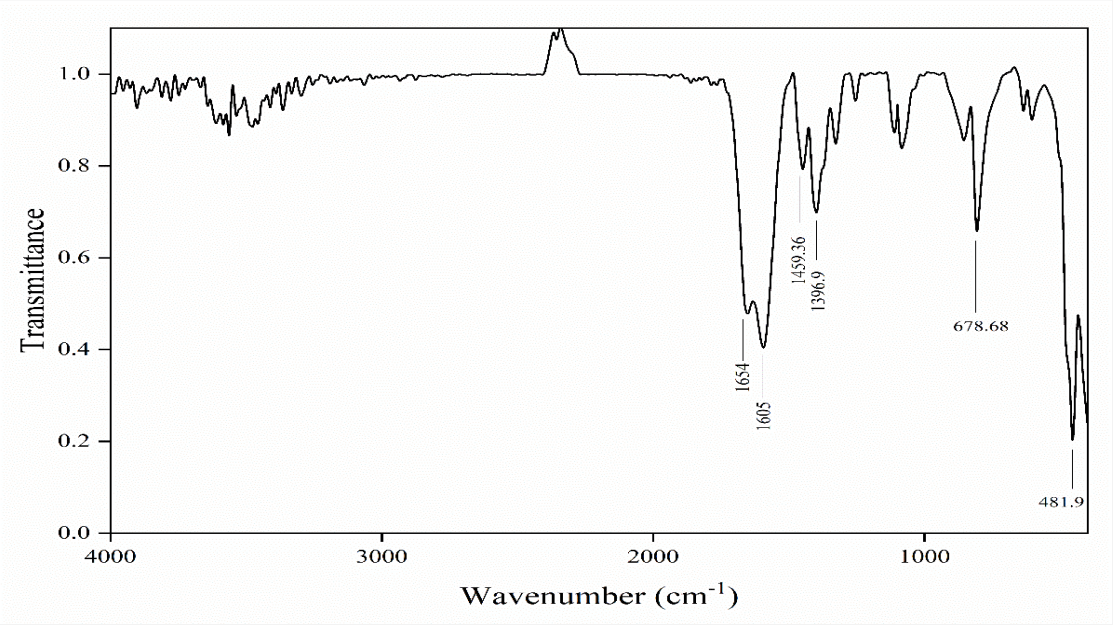

Figure 1. FT-IR Spectra of BMOF

3.2. Thermogravimetric analysis (TGA)

TGA was used to examine the Cu-Ni-EDTA Bimetallic MOF between 30 and 1000°C. A three-step weight drop was shown in Figure 2's BMOF thermogram. Ethanol and water loss between 31 and 75 degrees Celsius caused the first weight loss, which was roughly 6.1%. With a temperature range of 86 to 159°C, the DMF solvent evaporated, resulting in the second weight loss, which was calculated to be 5.19 percent. The third loss, or roughly 69.9%, was caused by the decomposition of the organic linker in MOF and the temperature range of 184 to 407°C. Ultimately, what was left behind was a black powder that contained nickel and copper oxide.

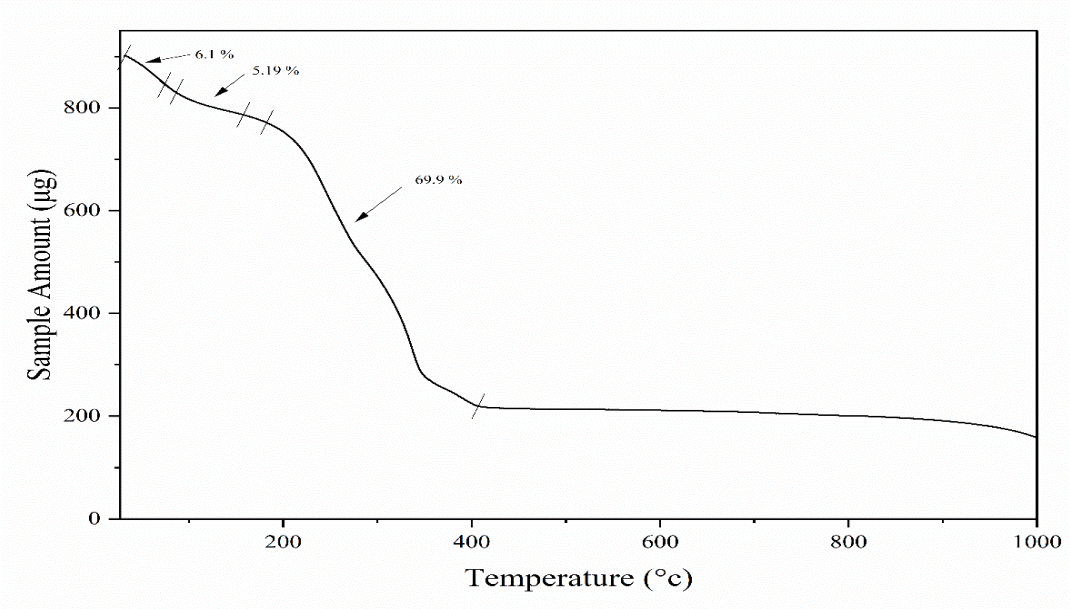

Figure 2. TGA Thermogram of BMOF

3.3. Field emission scanning electron microscopy-energy dispersive x-ray spectroscopy (FESEM-EDX)

The FESEM images presented in Figure 3(a-d) exhibit unique morphology, suggesting the existence of open pores on the surface of the structure. The copper and nickel metals are present in Figure 4's EDX Spectra and Figure 5's EDX mapping (a–f), respectively, with percentages of 20% and 8%. The elements carbon, nitrogen, and oxygen are also visible in the spectrum, with percentages of 41%, 8%, and 22%, respectively. The particle size ranges from 100 nm to 0.900 µm based on the SEM pictures.

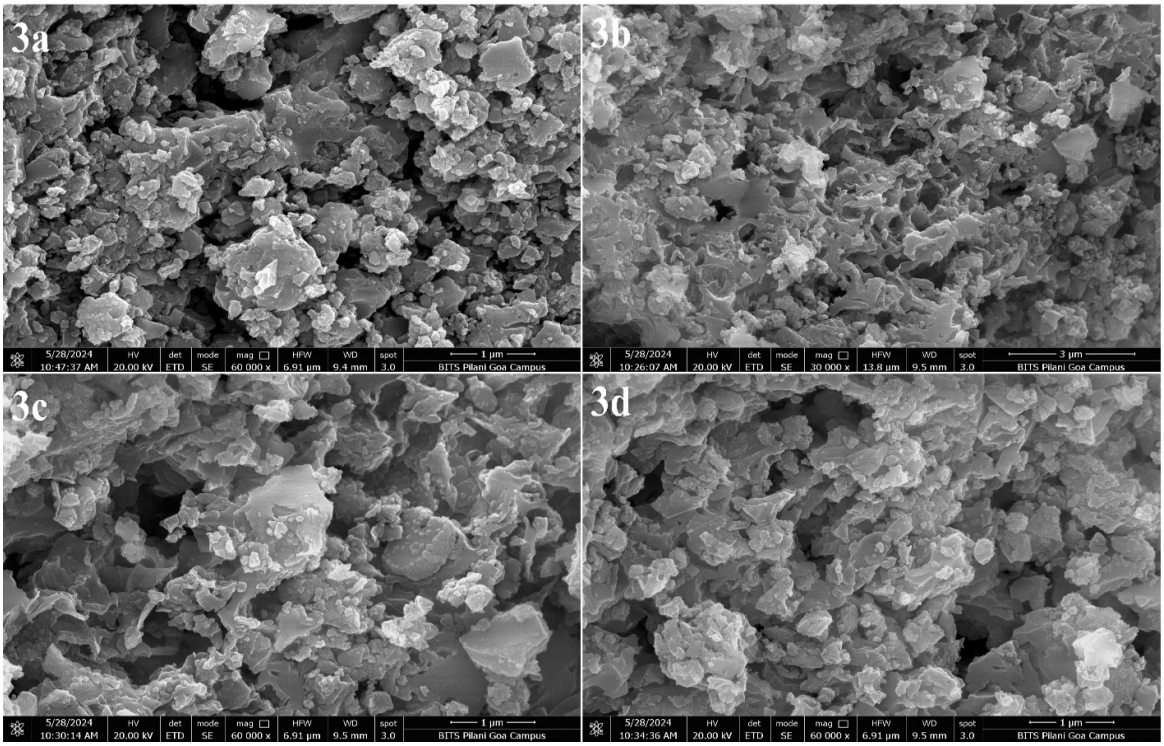

Figure 3. a, b, c and d are the FESEM images of BMOF

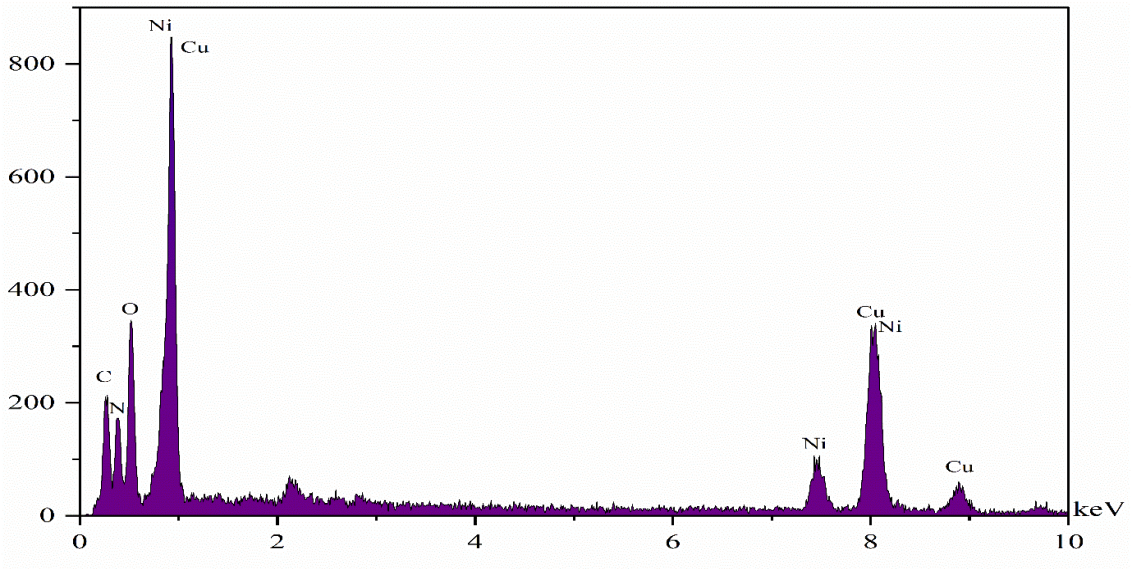

Figure 4. EDX Spectra of BMOF

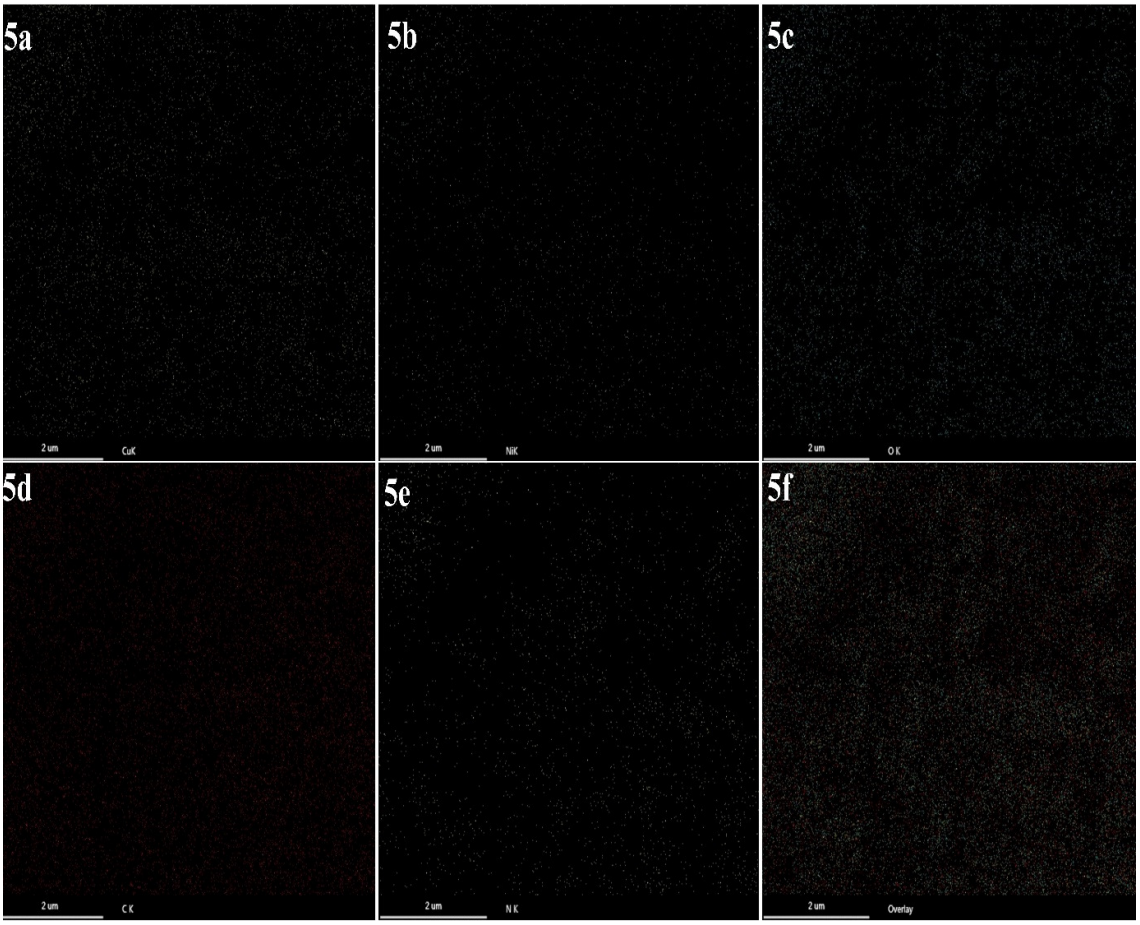

Figure 5. EDX Mapping of BMOF (a) Cu, (b) Ni, (c) O, (d) C, (e) N and (f) Overlay

3.4. X-ray photoelectron spectroscopy (XPS)

The elements Cu, Ni, O, N, and C found in our BMOF are further shown by the XPS spectra shown in Figure 6. Cu $2p_3$ and Cu $2p_1$ both contain copper, with concentrations of 932 and 952 eV, respectively. Additionally present at 941 and 568 eV, respectively, are Cu 2p and Cu Auger. At 872 eV, Ni $2p_1$ is visible, at 854 eV is the peak of Ni $2p_3$ and at 648 eV is Ni Auger. The sharp O 1s peak is visible at 529 eV, the sharp N 1s peak at 397 eV, and the sharp C 1s peak at 283 eV.

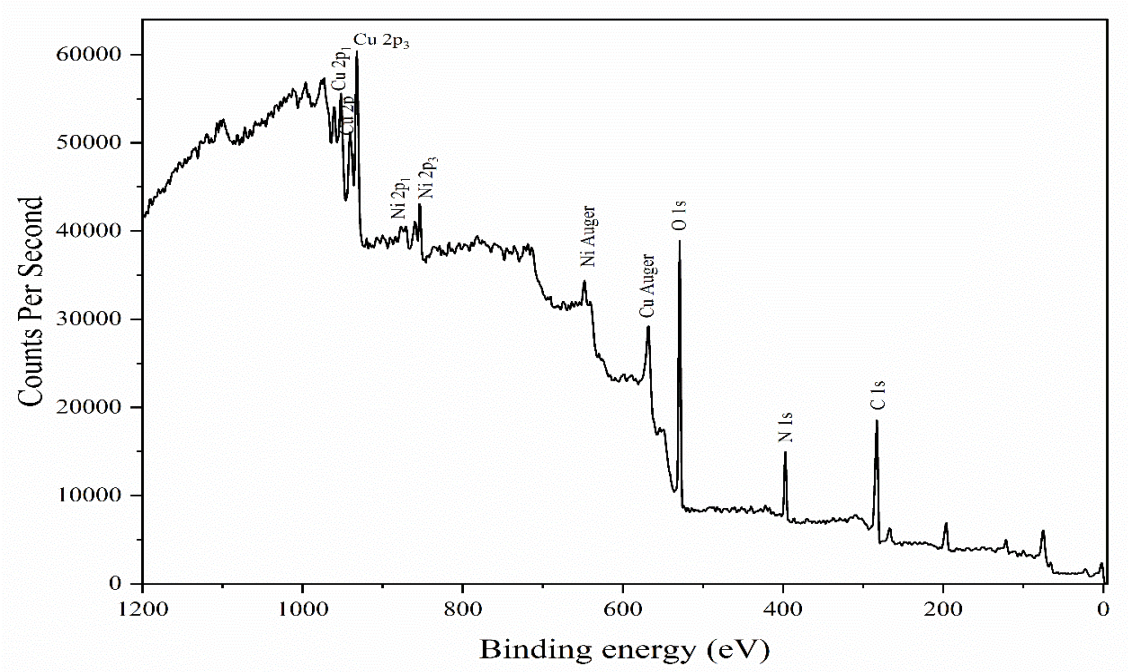

Figure 6. XPS Spectra of BMOF

3.5. Powder x-ray diffraction (PXRD)

To the best of my knowledge, the PXRD pattern depicted in Figure 7 is novel as it is the first time that the Cu-Ni-EDTA Bimetallic MOF has been produced. The complex Cu-EDTA is present at the peaks at 16.3º and 32.4º, as evidenced by the corresponding hkl planes of (001) and $(0\bar{1}3)$ [27]. The peaks at 39.8º with hkl plane of (111) indicates that the Ni is not in metallic (since its peak is at 44.5º) form as well as it is not in nickel oxide (because NiO peak is at 37.2º) form, which says that the Ni can be bonded with the EDTA [28]. The further peaks at 50º to 70º show that Cu-Ni bimetallic nature [29]. The Synthesized Bimetallic MOF's crystallinity is demonstrated by the sharp peak at 16.3º, 32.4º and 39.8º Debye Scherer's Equation (1) was utilized to compute the mean crystallite size:

$$D = \frac{0.9\lambda}{FWHMCos\theta} \quad (1)$$

where θ is the reflection angle, λ is the X-ray wavelength, and FWHM is the angle full width at half maximum Bragg peak. Scherer's equation yielded an average crystallite size estimate of 4.9136 nm.

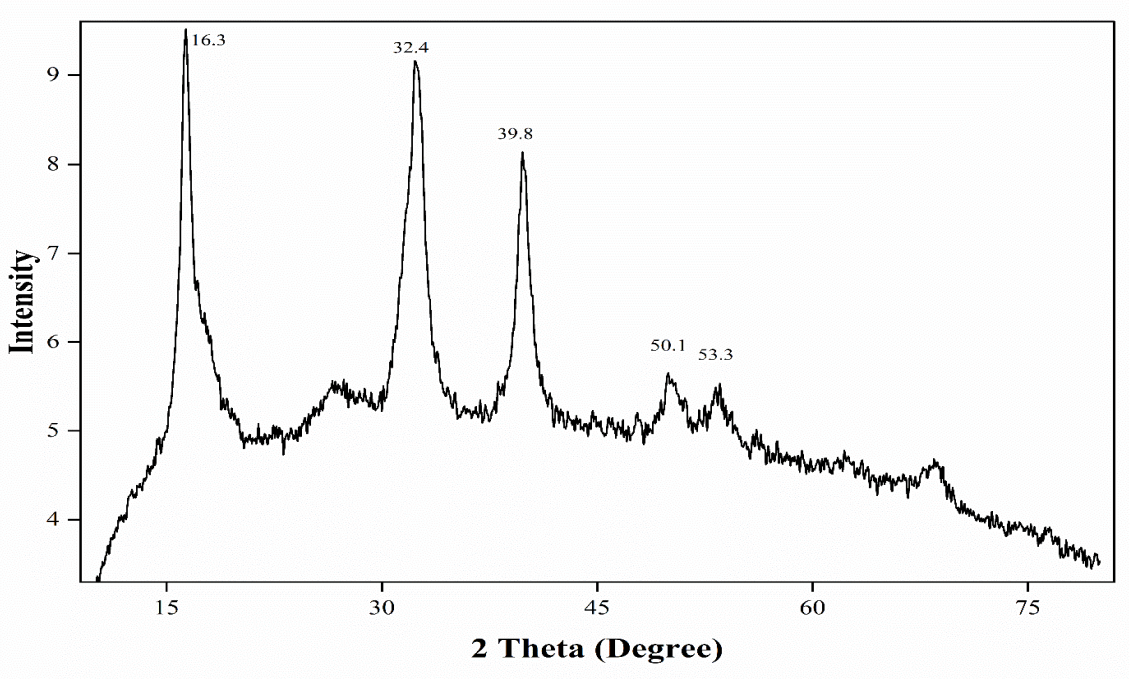

Figure 7. PXRD Pattern of the BMOF

3.6. Brunauer-Emmett-Teller (BET)

The specific surface area and pore size distribution of the generated Cu-Ni-EDTA Bimetallic MOF (BMOF) sample were ascertained by means of the N_2 gas adsorption/desorption isotherms derived from the Brunauer-Emmett-Teller (BET) gas-sorption experiments. Figure 8 shows the type IV N_2 adsorption–desorption isotherm according to the IUPAC classification of BMOF. The BMOF's BET specific surface area was found to be 293.14 m^2/g and its average pore diameter was found to be 3.84119 nm.

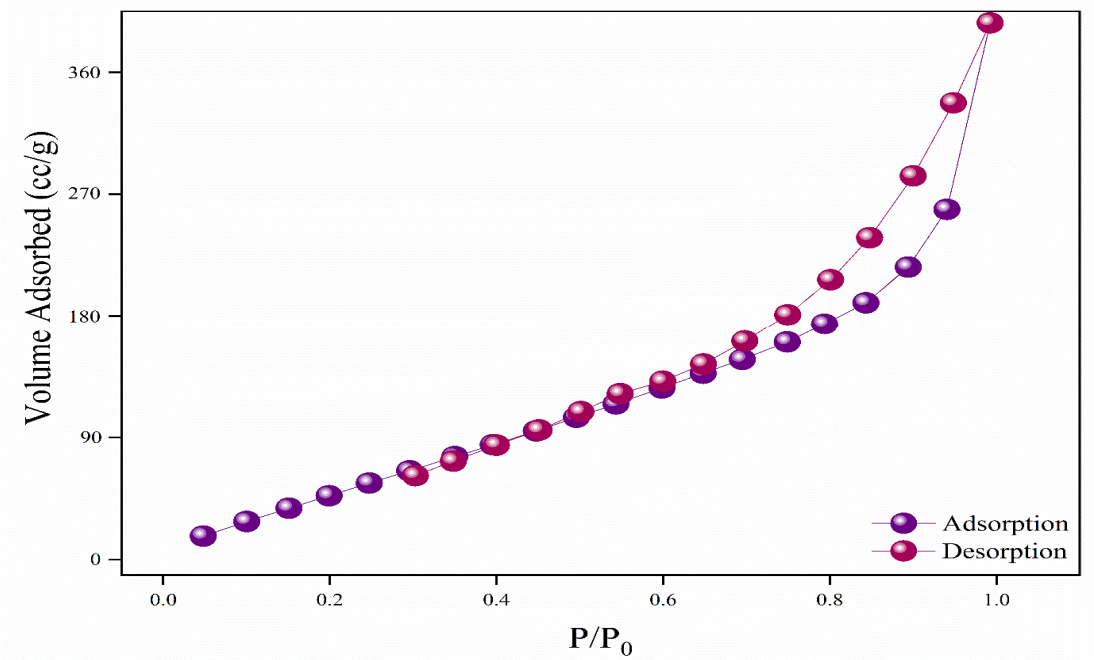

Figure 8. N_2 Adsorption/Desorption Isotherms of the BMOF

3.7. Antibacterial activity

In a 500 mL conical flask, Muller Hinton Agar Medium (High-Media) was dissolved in water, autoclaved at 121°C for 15 minutes at 15 pounds, and then transferred into sanitized petri plates. The Agar Well Plate Method was used to assess the sample's antibacterial activity [30]. The agar plates were covered with inoculum using a sterilized cotton swab. Samples were dissolved in DMSO to test their antibacterial activity. Some liquid samples were then added directly, using prepared aliquots of the compound (100µl/mL, 50µl/mL and 10µl/mL). These were pipetted into wells that had already been inoculated with specific species, such as Salmonella typhi, E. coli, and Staphylococcus aureus (Table 1). The plates were then incubated for 24 hours at 37ºC in an incubator, and the diameter (mm) of the clear inhibitory zone that formed around the wells was measured (Figure 9).

Table 1. Antibacterial Activity of the BMOF Sample

Test Microorganism	Antibacterial Activity	
	Concentration (µl/mL)	Zone of Inhibition (mm)
Staphylococcus aureus (MTCC-3160)	Control	22
	10	7
	50	10
	100	16
Escherichia coli (MTCC-443)	Control	20
	10	8
	50	10
	100	15
Salmonella typhi (MTCC-8767)	Control	20
	10	8
	50	12
	100	18

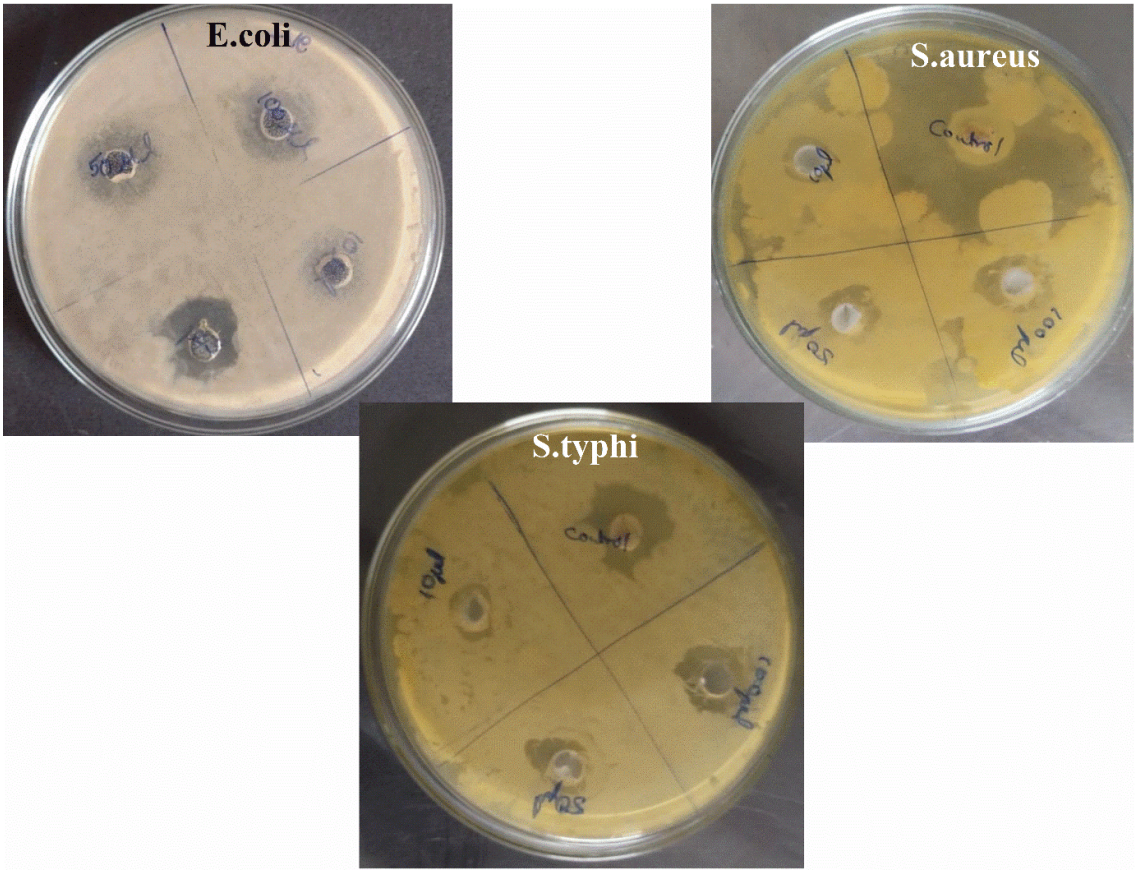

Figure 9. Antibacterial Activity of BMOF against E.Coli, S.aureus and S.typhi bacteria

4. Conclusion

Cu-Ni-EDTA Bimetallic MOF (BMOF) was effectively synthesized in this study utilizing a solvothermal technique, and it was then further characterized by FTIR, PXRD, FESEM-EDS, TGA, XPS and BET. The synthesized BMOF's crystallinity, morphological characteristics, thermal stability, and large surface area was shown by the characterization results. The EDS spectra is used to assess the purity of the synthesized BMOF. It reveals only the presence of the elements copper, nickel, carbon, nitrogen and oxygen as well as a distinct shape that suggests the presence of open pores on the structure's surface. Strong antibacterial activity of the synthesized BMOF was demonstrated against three types of bacteria: Salmonella typhi (MTCC-8767), Escherichia coli (MTCC-443) and Staphylococcus aureus (MTCC-3160).

Acknowledgement

The author gratefully acknowledges the Department of Chemistry at Andhra University for providing the essential facilities and instrumentation assistance for my research work. The author is also grateful to Advanced Analytical Laboratory of Andhra University, Indian Institute of Petroleum and Energy of Visakhapatnam, Indian Institute of Technology Hyderabad and the CSIF facility at the Birla Institute of Technology & Science of Pilani K K Birla Goa campus for doing the Thermogravimetric Analysis, Powder X-ray Diffraction Analysis, X-ray Photoelectron Spectroscopy Analysis and Field Emission Scanning Electron Microscopy-Energy Dispersive X-ray Spectroscopy Analysis respectively for my BMOF Sample.

References

[1] B. Desye, "COVID-19 Pandemic and Water, Sanitation, and Hygiene: Impacts, Challenges, and Mitigation Strategies", Environmental Health Insights., 15, ***(2021),*** *11786302211029447.*

[2] D. Ghernaout, A. Alghamdi and B. Ghernaout, "Microorganisms' Killing: Chemical Disinfection vs. Electrodisinfection", Applied Engineering., 3, 1, ***(2019),*** *13-19.*

[3] J. M. Boyce, "Modern technologies for improving cleaning and disinfection of environmental surfaces in hospitals", Antimicrob. Resist. Infect. Control., 5, ***(2016),*** *10.*

[4] N. J. P. Wawryk, C. B. Craven, L. K. J. Blackstock and X. F. Li, "New methods for identification of disinfection byproducts of toxicological relevance: Progress and future directions", J. Environ. Sci., 99, ***(2021),*** *151–159.*

[5] J. Walker, C. Chaguza, N. D. Grubaugh, M. Carey, S. Baker, K. Khan, I. I. Bogoch and V. E. Pitzer, "Assessing the global risk of typhoid outbreaks caused by extensively drug resistant Salmonella Typhi", Nat. Commun., 14, ***(2023),*** *6502.*

[6] M. A. Croxen, R. J. Law, R. Scholz, K. M. Keeney, M. Wlodarska and B. B. Finlay, "Recent advances in understanding enteric pathogenic Escherichia coli", Clin. Microbiol. Rev., 26, ***(2013),*** *822–880.*

[7] S. Jarraud, C. Mougel, J. Thioulouse, G. Lina, H. Meugnier, F. Forey, X. Nesme, J. Etienne and F. Vandenesch, "Relationships between Staphylococcus aureus genetic background, virulence factors, agr groups (alleles), and human disease", Infect. Immun., 70, ***(2002),*** *631– 641.*

[8] I. Roca, M. Akova, F. Baquero, J. Carlet, M. Cavaleri, S. Coenen, J. Cohen, D. Findlay, I. Gyssens, O. E. Heure, G. Kahlmeter, H. Kruse, R. Laxminarayan, E. Liébana, L. López-Cerero, A. MacGowan, M. Martins, J. Rodríguez-Baño, J.-M. Rolain, C. Segovia, B. Sigauque, E. Tacconelli, E. Wellington and J. Vila, "The global threat of antimicrobial resistance: Science for intervention", New Microbes and New Infections., 6, ***(2015),*** *22-29.*

[9] R. R. Marquardt and S. Li, "Antimicrobial resistance in livestock: advances and alternatives to antibiotics", Animal Frontiers., 8, 2, ***(2018),*** *30–37.*

[10] X. Zhang, F. Peng and D. Wang, "MOFs and MOF-Derived Materials for Antibacterial Application", J. Funct. Biomater., 13, 4, ***(2022),*** *215.*

[11] H. Furukawa, N. Ko, Y. B. Go, N. Aratani, S. B. Choi, E. Choi, A. Ö. Yazaydin, R. Q. Snurr, M. O'Keeffe, J. Kim and O. M. Yaghi, "Ultrahigh porosity in metal-organic frameworks", Science., 329, 5990, ***(2010),*** *424–428.*

[12] L. Jiao, Y. Wang, H. -L. Jiang and Q. Xu, "Metal–Organic Frameworks as Platforms for Catalytic Applications". Adv. Mater., 30, 37, ***(2018),*** *1703663.*

[13] J. Yang and Y. -W. Yang, "Metal–Organic Frameworks for Biomedical Applications", Small 16, 10, ***(2020),*** *1906846.*

[14] B. Claes, T. Boudewijns, L. Muchez, G. Hooyberghs, E. V. Van der Eycken, J. Vanderleyden, H. P. Steenackers and D. E. De Vos, "Smart Metal-Organic Framework Coatings: Triggered Antibiofilm Compound Release", ACS Appl. Mater. Interfaces., 9, 5, ***(2017),*** *4440–4449.*

[15] E. Yilgor, I. I. Nugay, M. Bakan and I. Yilgor, "Antibacterial silicone-urea/organoclay nanocomposites", Silicon., 1, ***(2009),*** *183–190.*

[16] M. Y. Masoomi, A. Morsali, A. Dhakshinamoorthy and H. Garcia, "Mixed-Metal MOFs: Unique Opportunities in Metal–Organic Framework (MOF) Functionality and Design", Angew. Chem. Int. Ed., 58, 43, ***(2019),*** *15188–15205.*

[17] A. Dhakshinamoorthy, A. M. Asiri and H. Garcia, "Mixed-metal or mixed-linker metal organic frameworks as heterogeneous catalysts", Catal. Sci. Technol., 6, ***(2016),*** *5238–5261.*

[18] Z. Li, M. Junaid, G. Chen and J. Wang, "Interactions and associated resistance development mechanisms between microplastics, antibiotics and heavy metals in the aquaculture environment", Rev. Aquac., 14, 2, ***(2022),*** *1028–1045.*

[19] C. D. Vecitis, K. R. Zodrow, S. Kang and M. Elimelech, "Electronic-structure-dependent bacterial cytotoxicity of single-walled carbon nanotubes", ACS Nano., 4, 9, ***(2010),*** *5471–5479.*

[20] J. Liu, D. Wu, N. Zhu, Y. Wu and G. Li, "Antibacterial mechanisms and applications of metal-organic frameworks and their derived nanomaterials", Trends Food Sci. Technol., 109, ***(2021),*** *413–434.*

[21] L. Argueta-figueroa, R. A. Morales-luckie, R. J. Scougall-vilchis and O. F. Olea-Mejía, "Synthesis, characterization and antibacterial activity of copper, nickel and bimetallic Cu–Ni nanoparticles for potential use in dental materials", Prog. Nat. Sci. Mater. Int., 24, 4, ***(2014),*** *321–328.*

[22] J. Yan, J. Li, P. Liu, H. Huang and W. Song, "Enhanced ammonia selectivity on electrochemical nitrate reduction: Cu–Ni metal–organic frameworks with tandem active sites for cascade catalysis", Green Chem., 25, ***(2023),*** *8645-8651.*

[23] G. Guo, "Direct fabrication of mixed metal–organic frameworks (Ni/Cu-MOF) and C@$NiCu_2O_4$ onto Ni foam as binder-free high performance electrode for supercapacitors", J. Mater. Sci: Mater. Electron., 32, ***(2021),*** *16287-16301.*

[24] S. Gopi, A. M. Al-Mohaimeed, W. A. Al-onazi, M. S Elshikh and K. Yun, "Metal organic framework-derived Ni-Cu bimetallic electrocatalyst for efficient oxygen evolution reaction", J. King Saud Univ.-Sci., 33, 3, ***(2021),*** *101379.*

[25] S. Momin, T. Mahmood, A. Ullah, A. Naeem and A. Khan, "Facile Synthesis of Cu–Zn Bimetallic MOF: Application as Superior Adsorbent for Effective Removal of Methylene Blue from Aqueous Solutions", Arab. J. Sci. Eng., 49, ***(2024),*** *9269-9290.*

[26] D. T. Sawyer and P. J. Paulsen, "Properties and Infrared Spectra of Ethylenediaminetetraacetic Acid Complexes. II. Chelates of Divalent Ions", J. Am. Chem. Soc., 81, 4, ***(1959),*** *816-820.*

[27] R. Manimekalai and C. R. Raja, "EDTA effect on Copper Sulphate Penta Hydrate-A NLO Material", Inte. Rese. J. Pure Appl. Chem., 3, 4, ***(2013),*** *391-403.*

[28] J. T. Richardson, R. Scates and M. V. Twigg, "X-ray diffraction study of nickel oxide reduction by hydrogen", Applied Catalysis A: General., 246, 1, ***(2003),*** *137-150.*

[29] C. Yang, W. Xue, H. Yin, Z. Lu, A. Wang, L. Shen and Y. Jiang, "Hydrogenation of 3-nitro-4-methoxy-acetylaniline with H_2 to 3-amino-4-methoxy-acetylaniline catalyzed by bimetallic copper/nickel nanoparticles", New J. Chem., 41, ***(2017),*** *3358-3366.*

[30] C. Perez, M. Pauli and P. Bazerque, "An antibiotic assay by the agar well diffusion method", Acta Biol. Med. Exp., 15, ***(1990),*** *113-115.*